CrossMark

Surface Microstructure of Mo(C)N Coatings Investigated by AFM

T. Kuznetsova, T. Zubar, S. Chizhik, A. Gilewicz, O. Lupicka, and B. Warcholinski

MoCN coatings have been formed by cathodic arc evaporation using the mixture of acetylene and nitrogen and pure molybdenum target. The surface structure, in conjunction with x-ray data, was analyzed by atomic force microscopy (AFM). The AFM results show differently shaped grain forms on the surface of coatings investigated. The increase in carbon in chemical coatings composition results in the reduction in surface grain size and the increase in roughness of the coatings.

1. Introduction

One of the ways to improve mechanical and tribological tools' and machine parts properties is surface's modification by a thin hard coating deposition. The properties of two-component coatings are often not able to meet the users' requirements. They can be improved, for example by changing the chemical composition (adding the third or more elements to two-element system) or by changing the coating structure by the choice of process parameters. In the latter case, for example, grain refinement (Ref 1) or forming the nanostructured composite coatings may occur (Ref 2). Such coatings may show low coefficient of friction, high wear resistance and high hardness.

Transition metals nitrides and carbides formed using PVD methods show good tribological and mechanical properties, including high hardness, low coefficient of friction, excellent wear and corrosion resistance, as well as characteristic color. For this reason, they are widely used as protective and decorative coatings (Ref 3-6). One of them is molybdenum nitride. High hardness and good adhesion, low coefficient of friction especially at higher temperature (Ref 7) and low wear rate make the coating a good candidate for the wide range of tribological applications.

Dependent on the chemical composition in Mo-N system, the existence of the following phases can be expected: space-centered cubic lattice of molybdenum Mo [JCPDS 42-1120], tetragonal-centered cubic phases: β-Mo$_2$N [JCPDS 24-0768], β'-Mo$_2$N [JCPDS 25-1368], β''-Mo$_2$N [JCPDS 75-1150], cubic γ-Mo$_2$N [JCPDS 25-1366], hexagonal δ-MoN [JCPDS 25-1367] and cubic phase marked B1 MoN (Ref 8). The tetragonal phases β-Mo$_2$N are low-temperature variations of the γ-Mo$_2$N

cubic phase. Due to different crystallographic structures, the phases exhibit different physical properties.

Studies on the effects of small amounts of elements such as C, Si, Cu, B, and others on the mechanical and tribological properties of CrN and TiN coatings have shown that such coatings have higher hardness and lower coefficient of friction (Ref 9-11). Carbon as a further component of the coating causes the change in morphology of the coating, but also affects the sliding behavior due to its low-friction properties.

Molybdenum carbide except for high hardness (Ref 12), corrosion resistance and high thermal stability also show catalytic properties (Ref 13). Zhao et al. (Ref 14) reported that carbon addition to MoCN enables to obtain nanomaterials with reduced grain size, dense active sites and high surface area. Some of above findings were confirmed by Liu et al. (Ref 12).

The properties of Mo-C-Si-N quaternary compositions (Ref 15) depend on carbon concentration. With the increase in C concentration, the average coefficient of friction and grain size decreases, while the hardness increases. Authors conclude that carbon atoms substitute nitrogen atoms in the nano-sized crystalline Mo$_2$N to form Mo$_2$N(C) solid solution phase. They also suggest that in the amorphous SiN$_x$ and CN$_x$ phases nano-sized crystalline Mo$_2$N(C) may be embedded.

The investigations of MoCN-Ag coatings (Ref 16, 17) indicate that the self-lubricating coatings significantly reduce the coefficient of friction, especially at elevated temperature, above 400 °C due to formation of molybdenum oxide and silver molybdate. A free amorphous carbon phase is responsible for low coefficient of friction up to 100 °C.

The properties of materials depend on their structure and microstructure determined by the chemical composition, the atomic structure of constituent phases. The microstructure can be modified by the technologies of production and the material processing. Therefore, the design and the production of new materials should be in control with their microstructure in order to assess the requirements compatibility with the result of the manufacturing process. This allows to detect both their formation mechanism and their behavior during operation. The method of atomic force microscopy (AFM) meets high requirements for investigation of thin vacuum coating deposited on polished substrates (Ref 18, 19). It allows not only to investigate topography of coating surface with nanometer resolution but also to detect heterogeneity in tribological surface properties caused by the presence of different phases in the coating.

T. Kuznetsova, T. Zubar, and **S. Chizhik**, A. V. Luikov Heat and Mass Transfer Institute of the National Academy of Sciences of Belarus, Minsk, Belarus; and **A. Gilewicz, O. Lupicka, and B. Warcholinski**, Faculty of Technology and Education, Koszalin University of Technology, Koszalin, Poland. Contact e-mail: bogdan.warcholinski@tu.koszalin.pl.

Table 1 Relationship between acetylene flow rate, carbon concentration in the coatings (Ref 16) and denotation of the coatings

| C_2H_2 flow rate, sccm	Carbon concentration, at.%	Coating notation
0	0	$Mo_{0.68}N_{0.32}$
5	7.1	$Mo_{0.64}C_{0.07}N_{0.29}$
10	13.5	$Mo_{0.56}C_{0.14}N_{0.30}$
15	16.2	$Mo_{0.54}C_{0.16}N_{0.30}$
20	18.5	$Mo_{0.53}C_{0.19}N_{0.28}$

The aim of this work was to study the surface microstructure of Mo(C)N coatings using AFM technique. To the best of our knowledge, Mo(C)N coatings have not been investigated using mentioned technique.
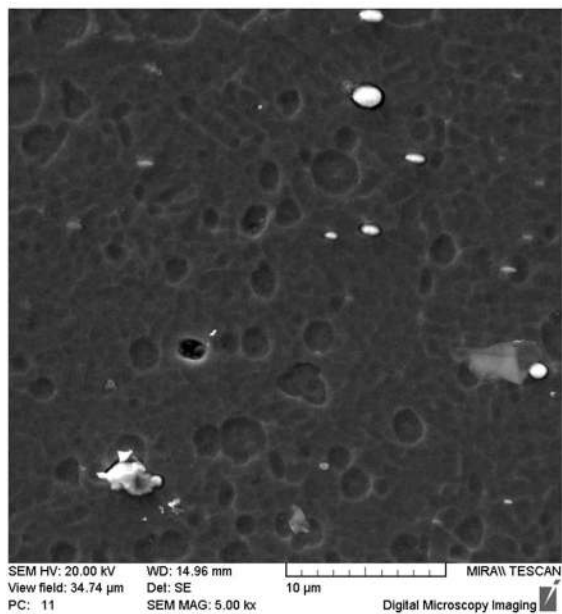
2. Experimental Details

Molybdenum carbonitride coatings were formed by introducing acetylene (C_2H_2) in the vacuum chamber of deposition system TINA 900M, using cathodic arc evaporation. All technological
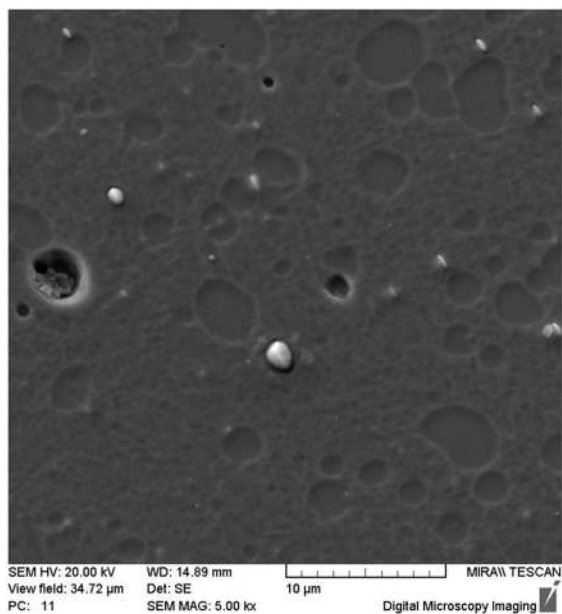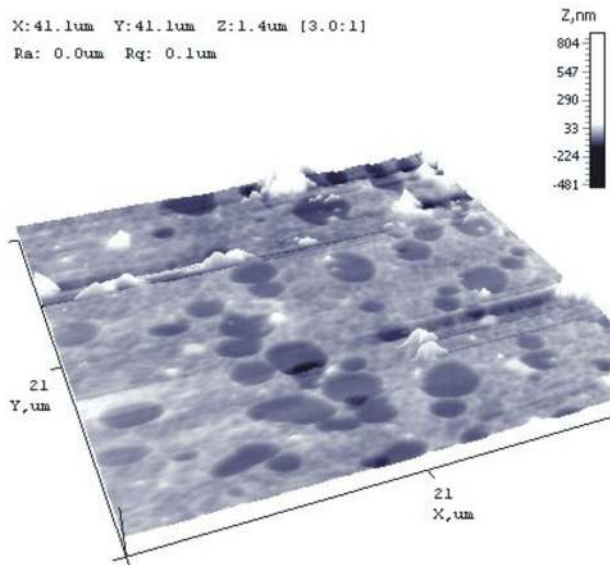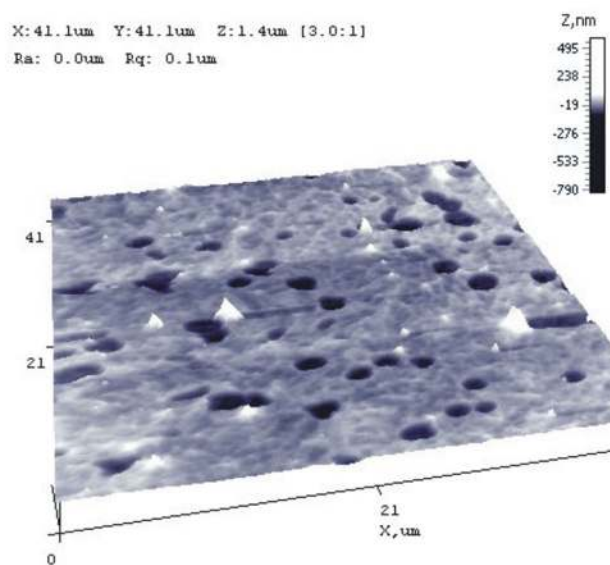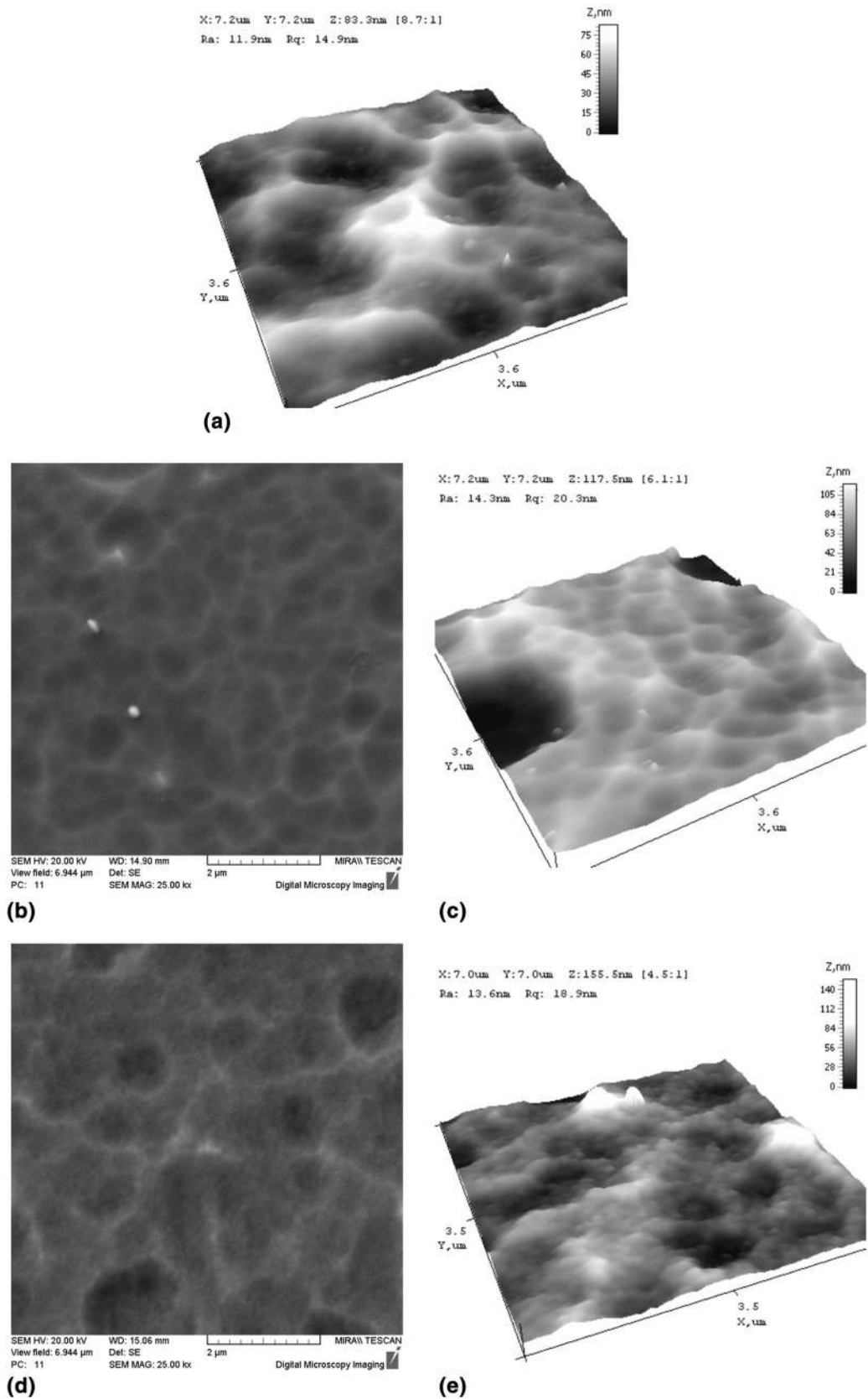

Fig. 1 Comparison of SEM and AFM microstructure of Mo(C)N coatings: (a) 7.1 at.% C, SEM, magnification ×5000; (b) 7.1 at.% C, AFM, scanning area 40 × 40 µm; (c) 18.5 at.% C, SEM, magnification ×5000; (d) 18.5 at.% C, AFM, scanning area 40 × 40 µm

Fig. 2 Comparison of SEM and AFM microstructure of Mo(C)N coatings on the area 7×7 μm: (a) 0 at.% C, AFM; (b) 7.1 at.% C, SEM; (c) 7.1 at.% C, AFM; (d) 18.5 at.% C, SEM; (e) 18.5 at.% C, AFM

Table 2   Roughness of Mo(C)N coatings investigated by AFM on the scanning area 40 × 40 μm

Flow of C_2H_2, sccm	Roughness, nm
0	27 ± 3
5	35 ± 5
10	31 ± 8
15	32 ± 2
20	38 ± 13

details and results of chemical composition investigations are shown in (Ref 20). The thickness Mo(C)N coating deposited on HS6-5-2 steel substrates is about 3 μm. The relationship between the flow of C_2H_2 in vacuum chamber and the carbon concentration in Mo(C)N coatings is presented in Table 1.

The investigation of topography of Mo(C)N coating using atomic force microscopy (AFM) was provided on NT-206 device (produced by MTM Belarus). As a result of scanning the surface in contact regime, two types of data are recorded in two different files: a normal deflection of cantilever and a cantilever twist. The normal deflection arises because of the surface relief. The twist of cantilever arises because of present forces between the surface and the tip (Ref 21). The normal deflection forms the topography image. The lateral projection of cantilever twist forms the image of lateral forces named "Torsion." The main part of the lateral forces is friction force. Friction force is joined effect of elasticity, adhesion, viscosity, capillary forces, surface chemistry, electrostatic interaction and so on. The first or the second phenomenon occurs dependent on the conditions and material dominated. So the cantilever twist is caused by surface properties. This "Torsion" regime can be used for a distinction of different phases in Mo(C)N as a phase is a region of space in which all physical properties of a material are uniform. The phase according to AFM is a region of the surface with a boundary which has the same color. One color means one angle of cantilever twist. The value of cantilever twist depends on cantilever stiffness. The silicon cantilevers of CSC 38 type (Micromasch, Estonia) with stiffness coefficient $k = 0.08$ N/m were used in this research. The phases recorded using AFM were compared with phases recorded and identified in x-ray diffraction (XRD). AFM gives a map of the surface with particles and regions of different colors (white, gray, dark). x-ray analysis helps to choose the possible chemical formula of the phase. As the silicon cantilever is very sensitive, it is possible to discriminate more phases on the thin coating surface than according to XRD. The roughness measurements were conducted on five randomly selected areas.

Preliminary tests of wear using AFM equipped in diamond tip with radius about 200 nm were performed on selected coatings on the scan area 5×5 μm² with load about 2 mN, 3 scans at the same place, 128 lines in scan and average scan velocity about 14.8×10^{-6} m/s. The specific wear rate was calculated according to Archard's formula.

Surface microstructure was investigated using scanning electron microscope "Mira" produced by Tescan (Czech Republic).

3. Results and Discussion

The high-resolution method of scanning electron microscopy (SEM) does not allow significant differentiation in the microstructure of the Mo(C)N coatings obtained with different volume of acetylene in the vacuum chamber. The main structural features of these coatings at the magnification of ×5000 are microdroplets, craters after chipping of microdrops, spherical particles of oxides (Fig. 1).

The fraction of microdroplet phase in Mo(C)N coatings amounts to several percent, and it does not manage to determine the differences according to this criterion. When assess the microstructure of coating surface according to SEM images with magnification of ×25000, it is only possible to make conclusion that protruding borders of cells are the most developed and have the smallest cells size about 600 nm for the coating with 7.1 at.% of carbon. In coating with 13.5 at.% C, the borders are poorly visible. The developed borders in this coating are very rare. In coating with 18.5 at.% C, the borders achieve the biggest size of about 1 μm (Fig. 2).

The use of AFM on the scanning field with size from 20×20 μm till 40×40 μm enables to assess only the depth of craters after chipping of microdrops (Fig. 1b and d). It is 50-120 nm. Like in SEM images, in AFM images the largest crater diameters of about 5 μm are in the coating obtained with 5 sccm acetylene flow. The smallest crater diameters of about 2 μm are in coating with 20 sccm C_2H_2 flow. The coatings obtained with 10 and 15 sccm acetylene flow have irregular distribution of craters (Fig. 1b and d).

The values of roughness Mo(C)N coatings obtained by AFM on areas 40×40 μm are in Table 2. It should be noted that roughness determined using AFM technique for Mo(C)N coating deposited without acetylene flow rate in the same technological conditions is similar. For $Mo_{0.68}N_{0.32}$ Ra was determined using contact recording instrument (Hommel Werke T8000) and amounts to about 0.04 μm (Ref 22).

But in the case of AFM, undetected features of the coating which is formed under C_2H_2 flow are only the problem of the right size scanning area selection. The use of the scanning area 5×5 μm enabled to register the difference in the microstructure of Mo(C)N coating formed at different acetylene flow rate in vacuum chamber (Fig. 3). That difference reflects the influence of the main deposition parameters and mainly the energy of bombardment on the coating formation. Two competing processes occur—deposition and resputtering of the coating. As an effect of resputtering are well-shaped cavities. The border of grain as a more harder material is resputtered slower than the softer body of grains. During the ion bombardment, the atoms from horizontal surfaces are resputtered easier than the atoms from vertical surfaces. Therefore the surface obtained by AFM as 3D images is interpreted as a multi-cell structure in which lowered bottom of the cells (core grain) and elevated vertical grain boundaries are visible.

The microstructure of MoN coating obtained without acetylene consists of "cells" characterized by relatively large size—about 2 μm (Fig. 3a), completely randomly arranged. In coating deposited at 5 sccm C_2H_2 flow, the cells with smaller size, about 700 nm (Fig. 3b), are formed. The increased flow rate of the acetylene in the vacuum chamber results in additional carbon atoms which give rise in the number of crystallization nuclei on the surface of the formed coating. The density of the crystallization centers grows, and the formation of ridges is faster than without acetylene. The growing ridges form ordered cells of smaller size than without carbon. Around one cell, there are usually about six other cells. As a result, grains in size of about 100-200 nm appear in the microstructure of the coatings deposited with 10, 15, 20 sccm of acetylene
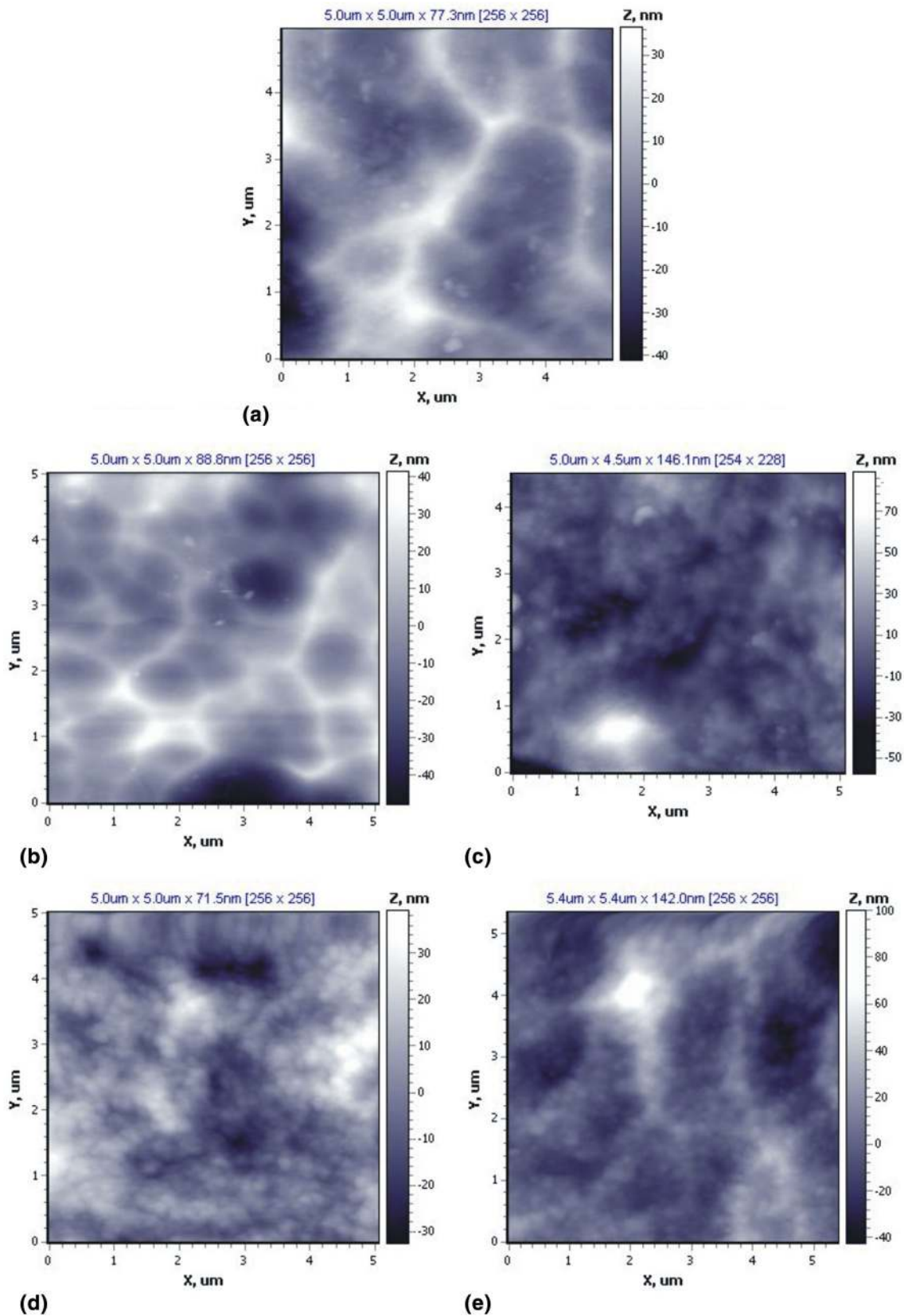
Fig. 3 AFM microstructure of Mo(C)N coatings, scanning area 5 × 5 μm: (a) 0 % at. C; (b) 7.1 at.% C; (c) 13.5 at.% C; (d) 16.2 at.% C; (e) 18.5 at.% C
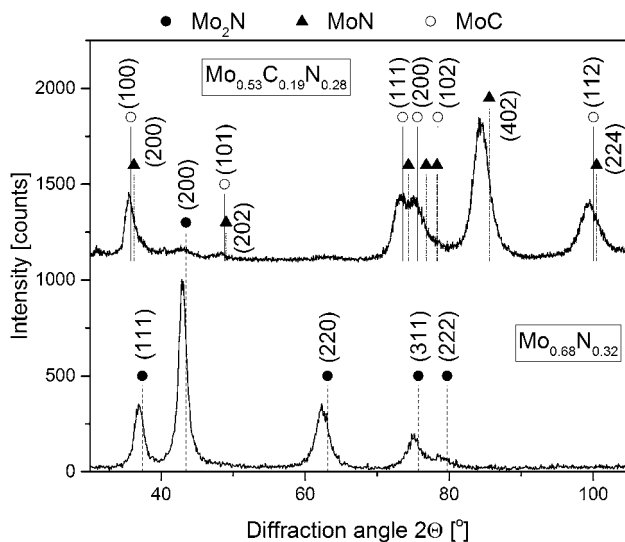
Fig. 4 XRD patterns of $Mo_{0.68}N_{0.32}$ and $Mo_{0.53}C_{0.19}N_{0.28}$ coatings formed using cathodic arc evaporation

flow. The carbon content increase in the coating leads to more ordered microstructure. In coating deposited at 10 sccm C_2H_2 flow, the grains are located randomly (Fig. 3c), but in coating deposited at 15 sccm C_2H_2 flow the fragments of linear chain of grains can be seen, Fig. 3(d). In coating obtained with 20 sccm C_2H_2 flow, small grains with diameter of 100-200 nm are located into border of grains sized in a range 0.5-1.5 μm (Fig. 3e). In this coating, the grains are ordered into the honeycomb-like structure.

The usage of AFM regime "Torsion" (or Lateral Forces) allows to visualize different phases on the surface of Mo(C)N coatings. The comparison of AFM data in "Torsion" regime with XRD data allows to get a distribution map of different phases in Mo(C)N coating (Ref 20).

According to the phase diagram and XRD results, the coating without carbon is characterized by cubic Mo_2N phase. But in the range of angles 72°-82°, some diffraction lines exist, which are broadened, shifted and overlay themselves (Fig. 4).

Despite the fact that according to the diffraction pattern on the surface of coating there are not any other phases, in AFM images (Fig. 5a) in the structure of MoN coating three types of phases can be visible: gray phase (indicator 1, Fig. 5a), which is both the background for white phase in size of about 100-400 nm (indicator 2, Fig. 5a) and dispersed black phase in size of about 50 nm (indicator 3, Fig. 5a). It can be supposed that the black phase is MoN. The white phase can be not quite stoichiometric phase or can be formed by some individual parts in the coating with the main cubic Mo_2N phase.

Based on the results (Ref 19) in which it was found that during nitriding of molybdenum in terms of saturation with nitrogen to temperature of 940 °C two layers: the outer layer of MoN and inner of Mo_2N were formed on the surface, we assume that fine black grains (phase) can be attributed to MoN. The same effect occurs in case of tungsten (Ref 23).

The existence of different phases on the coatings surface can be confirmed by findings of Yuan et al. (Ref 15) who suggest that carbon atoms substitute nitrogen atoms in the nano-sized crystalline Mo_2N to form $Mo_2N(C)$ solid solution phase.

In fact the C_2H_2 flow of 5 sccm during deposition does not change the phase composition of the coating. It leads to the

increase in formation of all nitride phases. Based on the intensity of the diffraction lines such as (111) expected at 33.38° for Cu-Kα radiation, (200) at 43.45° or (220) at 63.11° according to ICDD 25-1366 it can be stated that this coating consists mainly of the cubic Mo_2N phase. In contrast, the next diffraction line (311) positioned at 75.73° is more interesting. Its intensity increases and slightly broadens. It may be caused by the formation of MoC and/or MoN phase, but the amount of these compounds could be insufficient to be register by XRD. Such an increase in formation of nitride phases with the addition of small amount (5 sccm C_2H_2 flow) of carbon is reflected in the structure in form of grain size decrease, what is apparent in AFM image. The increase in carbon concentration in Mo(C)N coatings leads both to the appearance of larger crystallization centers quantity on the surface and to the decrease in grains size. In the microstructure of the surface, the grain size decrease is visualized in form of cells size decrease from 3 to 5 μm for molybdenum nitride coating without carbon (Fig. 3a) to 1-2 μm for molybdenum nitride coating with carbon amount of 7.1 at.% (C_2H_2 flow rate of 5 sccm), Fig. 3(b). There are also more developed ridges of grains in this coating. The quantity of ridges increases, and it leads to surface roughness rise from 29.3 to 46.5 nm on the area of 40×40 μm^2 (Table 1). In AFM "Torsion" regime, the quantity of phases, which are contrasted with the main phase, increases. Moreover, their size also decreases and the main phase is Mo_2N. In AFM image, the phase has gray contrast and consists of nanosized subgrains with diameter of 20-50 nm (indicator 1, Fig. 5b). As it was mentioned above, the diffraction lines are broadened and shifted to lower angles from their positions. It can be associated with the nanosized structure of coating. They are different in forms and color types of particles from the others phases in the background of main Mo_2N phase as dispersed dark particles with diameter of 20-50 μm so as lamellar bright particles with diameter 300-500 nm (indicator 2, Fig. 5b). They confirm the possibility of the existence of MoN and MoC phases (Fig. 4b). For the lamellar bright particles determined as MoC phase, the increase in size is more significant.

The addition into vacuum chamber 10 sccm C_2H_2 flow leads to the formation of significant quantity of MoC phase, which reaches the quantity of nitrogen phases. The deconvolution of complex and broadened diffraction lines in 2Θ angle range 70°-87° revealed the existence of MoN and MoC phases except for present Mo_2N phase. The quantity of the phases is approximately equal.

The ridges are visible (Fig. 3) for $Mo_{0.68}N_{0.32}$ and $Mo_{0.64}C_{0.07}N_{0.29}$ coatings which do not show carbon phases in XRD diffraction pattern, Fig. 5. The increase in carbon in Mo(C)N coatings decreases the grain size to about 100-200 nm (Fig. 3c). Such surface microstructure means that acetylene (source of carbon) introduced into the vacuum chamber has not only distributed on the surface in the form of crystallization nuclei, but its quantity is sufficient for stoichiometric MoC phase. In "Torsion" regime, there are dark particles dispersed, probably MoN (indicator 2, Fig. 5c) and white lamellar inclusions presumptive MoC phase (indicator 3, Fig. 5c). The first phase particles dimension is about 20-50 nm, and the white phase is about 400-600 nm. Based on observation of the microstructure in the lateral force regime, it can be noted that the number of phases in both colors increased. They are uniformly distributed on the surface.

The increase in the acetylene flow rate in the vacuum chamber to 15 sccm results in achieving the maximum intensity of MoC phase diffraction lines in the diffraction pattern. The
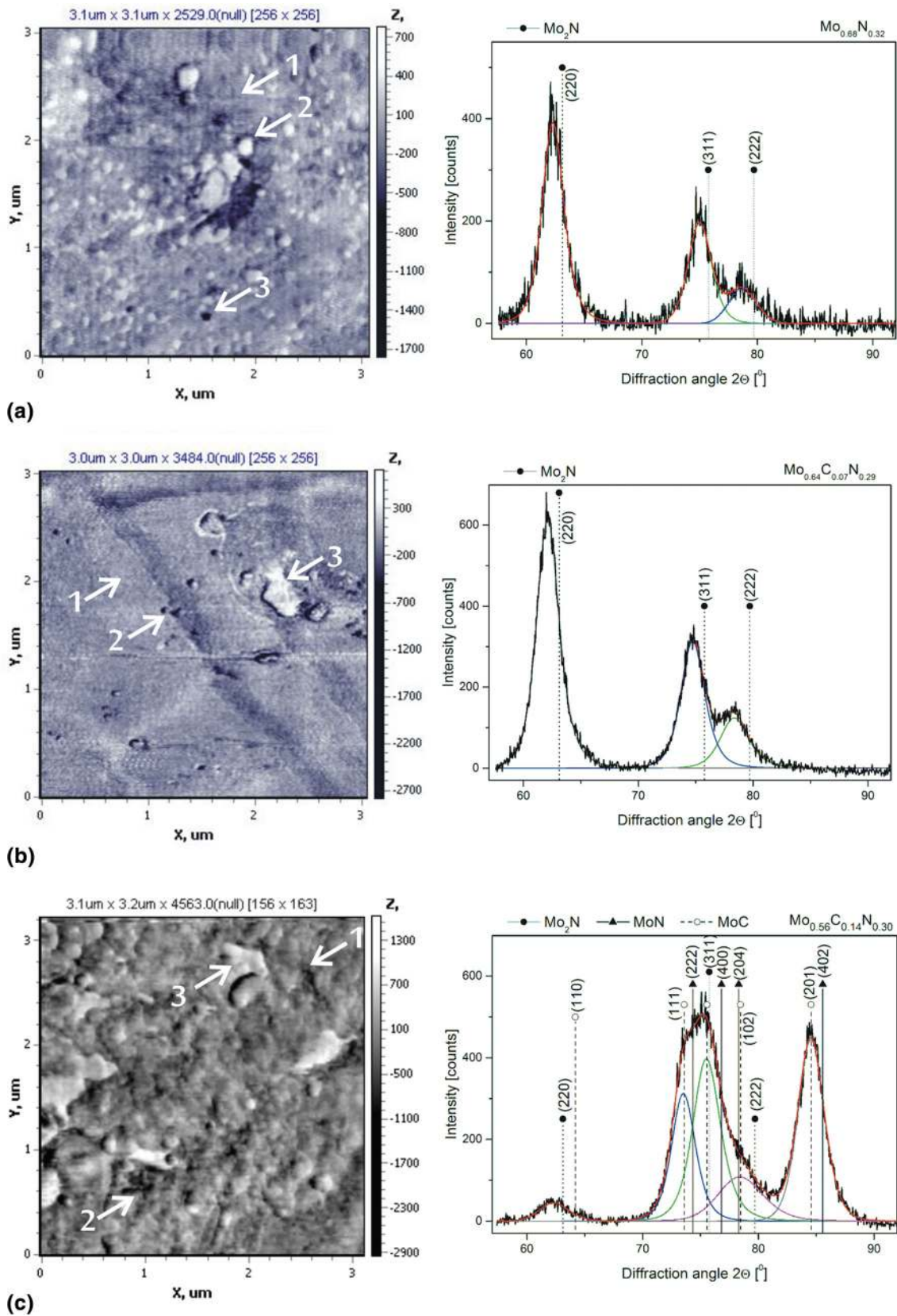
Fig. 5 Microstructure of Mo(C)N coatings with carbon obtained with AFM in ''Torsion'' regime, left side, compared with XRD dates, right side. Acetylene flow rate: (a) 0 sccm, (b) 5 sccm, (c) 10 sccm, (d) 15 sccm, (e) 20 sccm
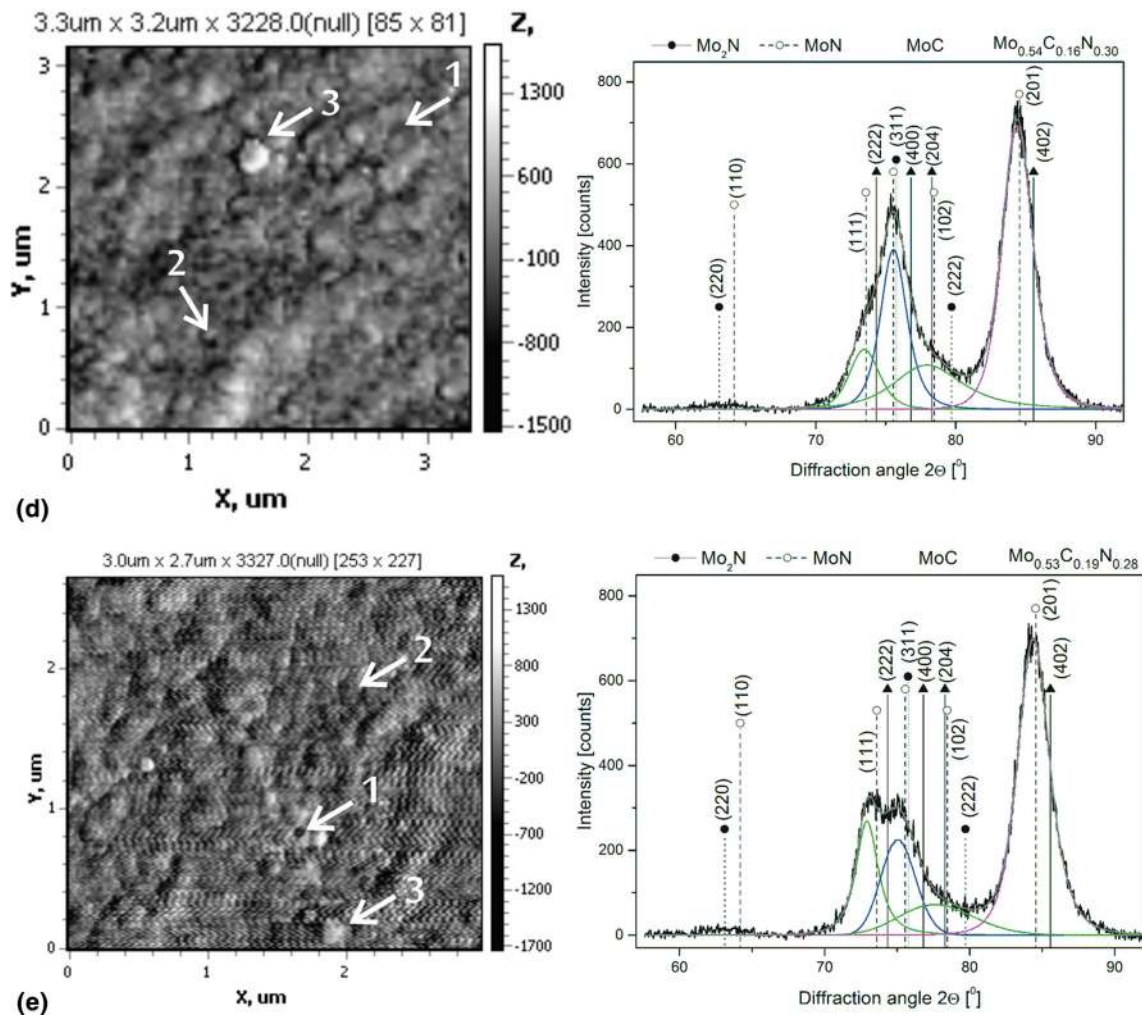
Fig. 5 continued

Table 3 Size of phases observed in AFM measurements

| | The size of phases | | | |
| | Mo$_2$N | | MoC | MoN |
Coating	Grains, μm	Sub-grains, nm	Grains, nm	Grains, nm
Mo$_{0.68}$N$_{0.32}$	2-5	100-200	…	20-50
Mo$_{0.64}$C$_{0.07}$N$_{0.29}$	0.5-1	50-100	…	20-50
Mo$_{0.56}$C$_{0.14}$N$_{0.30}$	0.1-0.2	…	400-600	20-50
Mo$_{0.54}$C$_{0.16}$N$_{0.30}$	0.1-0.2	…	100-400	30-50
Mo$_{0.53}$C$_{0.19}$N$_{0.28}$	0.1-0.2	…	100-200	50-100
			Size of cells 1-2 μm	

further rise of the acetylene flow rate to 20 sccm does not change intensity in MoC diffraction lines. Probably, the formation of MoC phase could be finished. A transformation of the main Mo$_2$N phase to mixture of Mo$_2$N, MoN and MoC phases takes place. The structure type is changing drastically (Fig. 5c). The dispersed phase appears fast in the coating with a uniform grain size of 100-200 nm (indicator 1, Fig. 5c). Bright and dark particles (indicator 2, Fig. 5c) are uniformly distributed on the surface. We suppose that lamellar bright

particles of MoC phase compared with one shown in Fig. 5(b) have more developed surface. Their size decreased significantly to 100-400 nm (indicator 3, Fig. 5c).

In the Mo$_{0.53}$C$_{0.19}$N$_{0.28}$ coating formed in vacuum chamber in acetylene flow rate of 20 sccm, the surface microstructure type, that is dispersed, grains do not change (Fig. 5e) and are the same as for coating formed in 15 sccm of acetylene. The difference is in grain size—in this coating they were decreased. The size of dark, probably MoN, dispersed phase is 50-100 nm
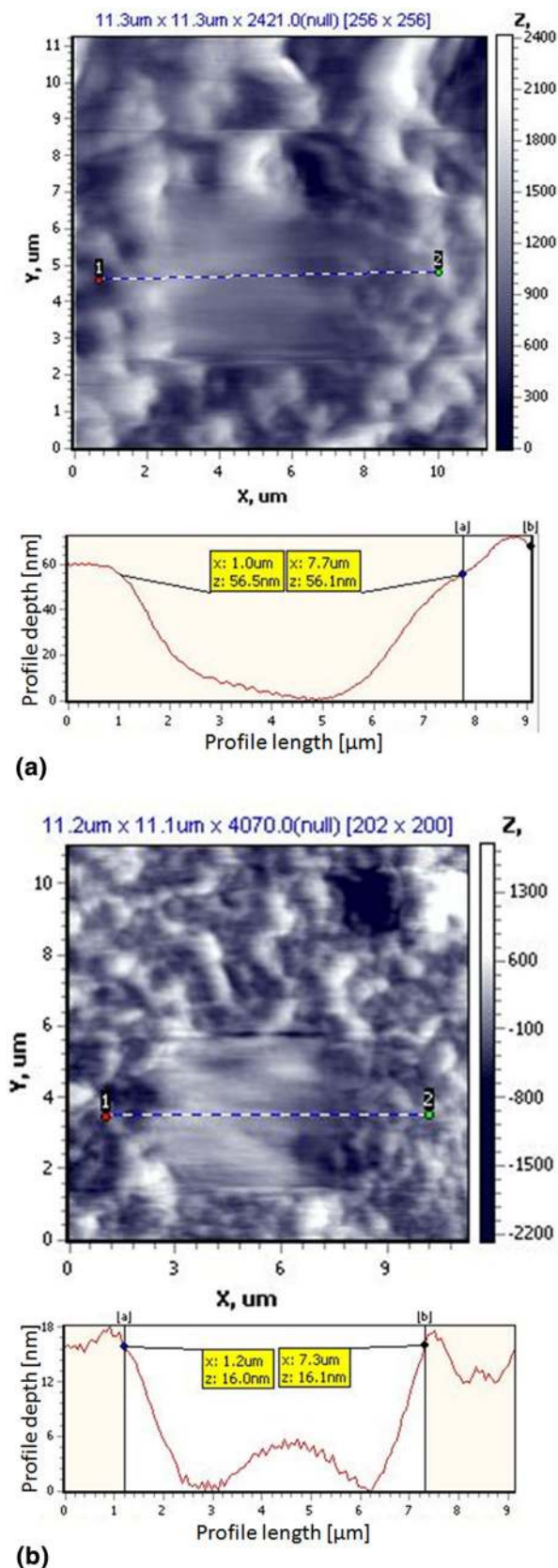
Fig. 6 Results of the wear and wear profile using AFM of: (a) $Mo_{0.68}N_{0.32}$ and (b) $Mo_{0.56}C_{0.14}N_{0.30}$ coatings. The dashed line (1-2) indicates the position of wear profile in wear area

(indicator 1, Fig. 5e). The other particles MoC (indicator 2, Fig. 5e) and Mo_2N (indicator 3, Fig. 5e) have similar size—100-200 nm. The main structure of dispersed particles is ordered. The grains are arranged into a honeycomb structure with a cell size of about 1 μm. The size of phases observed in AFM measurements in all coatings is gathered in Table 3.

Due to refinement of grains and for proper assessment of grain dimensions, the AFM measurements on the square 10×10 μm ought to be taken. The roughness resulted from these tests reflects the features of coating formation correctly. The features of microstructure of Mo(C)N coating like microdrops significantly affect the value of roughness on square 20×20 μm or more. Its surface distribution has a random nature. The smaller size of square causes incorrect cells structure. So the coating with 7.1 at.% C shows 19 nm roughness, while the common MoN coating is only 10 nm. This confirms an idea that at acetylene flow rate of 5 sccm in vacuum chamber, MoC phase does not form. Instead of that, the grain refinement of nitriding phases occurs and as an effect the more shaped grain boundaries are formed and the additional ridges appear on the surface. Therefore, the value of roughness decreases to 11.2 nm for coatings deposited at C_2H_2 flow rate of 10 sccm and to 9.4 nm at 15 sccm. The MoC phase formed as the rounded nanosized grains smoothes the coating surface. The further increase in roughness to 15.2 nm is connected with the appearance of chains and ridges from grains.

Hard coating shows usually high wear resistance, and as consequence the depth of wear tracks was several nanometers. The relief of the surface and craters were more apparent than the depth of obtained wear tracks. The results of wear tests on Mo_2N (acetylene flow rate—0 sccm) and Mo(C)N deposited using acetylene flow rate of 10 sccm are presented in Fig. 6. Below images of worn surface of the coatings the profiles of wear tracks are added.

The depth of wear (volume of material removed from the surface) was 56 nm (9.0×10^{-19} m^3) for Mo_2N coating and 16 nm (2.6×10^{-19} m^3) for Mo(C)N coating deposited using 10 sccm of acetylene. Specific wear rate calculated according to Archard's formula is 14.6×10^{-14} m^3/N m and 4.2×10^{-14} m^3/N m, respectively. It means that MoCN coatings can present better wear resistance compared to Mo_2N coating.

4. Conclusion

The presence of MoC phase is not observed for low carbon concentration in Mo(C)N coatings corresponding to acetylene flow rate of 5 sccm in vacuum chamber. This phase starts to form with higher than 5 sccm C_2H_2 flow rate and appears as the grain structure instead of cells structure. With further increase in the acetylene flow rate, the grain size in Mo(C)N coating decreases. In coatings deposited at C_2H_2 flow rate of 20 sccm, the grains form the ordered cell structure with the grain size of 100-200 nm and the cell size of 1 μm.

The phase composition of coatings changes with the increase in carbon concentration in Mo(C)N. The initial Mo_2N phase, which is characterized by cubic lattice, is replaced by hexagonal MoN and MoC phases. It seems the coatings with carbon have a better view tribological application. However, in-depth studies must be carried out to confirm this conclusion.

Acknowledgments

Open Access

References

1. S. Hogmark, S. Jacobson, and M. Larsson, Design and Evaluation of Tribological Coatings, *Wear*, 2000, **246**, p 20–33
2. J. Musil, Hard and Superhard Nanocomposite Coating, *Surf. Coat. Technol.*, 2000, **125**, p 322–330
3. Z. Peng, H. Miao, W. Wang, S. Yang, C. Liu, and L. Qi, Hard and Wear-Resistant Titanium Nitride Films for Ceramic Cutting Tools by Pulsed High Energy Density Plasma, *Surf. Coat. Technol.*, 2003, **166**, p 183–188
4. B. Navinsek, P. Panjan, and I. Milosev, Industrial Applications of CrN (PVD) Coatings, Deposited at High and Low Temperatures, *Surf. Coat. Technol.*, 1997, **97**, p 182–1891
5. P.H.M. Böttger, L. Braginsky, V. Shklover, E. Lewin, J. Patscheider, D.G. Cahill, and M. Sobiech, Hard Wear-Resistant Coatings with Anisotropic Thermal Conductivity for High Thermal Load Applications, *J. Appl. Phys.*, 2014, **116**, p 013507
6. P.H. Mayrhofer, R. Rachbauer, R. D. Holec, F. Rovere, and J.M. Schneider, Protective Transition Metal Nitride Coatings, in: S. Hasmi (Ed.) *Comprehensive Materials Processing*, Elsevier, Amsterdam, 2014, p 355–388
7. X. Zhu, D. Yue, C. Shang, M. Fan, and B. Hou, Phase Composition and Tribological Performance of Molybdenum Nitride Coatings Synthesized by IBAD, *Surf. Coat. Technol.*, 2013, **228**, p S184–S189
8. F. Perry, A.W. Baouchi, J.H. Petersen, and S.D. Pozder, *Surf. Coat. Technol.*, 1992, **54**(55), p 261–265
9. T. Polcar, L. Cvrček, P. Široký, and R. Novák, Tribological Characteristics of Cr(CN) Coatings at Elevated Temperature, *Vacuum*, 2005, **80**, p 113–116
10. L. Karlsson, L. Hultman, M.P. Johansson, J.E. Sundgren, and H. Ljungcrantz, Growth, Microstructure, and Mechanical Properties of Arc Evaporated TiC_xN_{1-x} ($0 \leq x \leq 1$) films, *Surf. Coat. Technol.*, 2000, **126**, p 1–14
11. J. Almer, M. Odén, and G. Håkansson, Microstructure, Stress and Mechanical Properties of Arc-Evaporated Cr-C-N Coatings, *Thin Solid Films*, 2001, **385**, p 190–197
12. Q. Liu, T. Liu, Q.F. Fang, F.J. Liang, and J.X. Wang, Preparation and Characterization of Nanocrystalline Composites Mo-C-N Hard Films, *Thin Solid Films*, 2006, **503**, p 79–84
13. G. An and G. Liu, Preparation of Ultramicro Molybdenum Carbide Powders and Study on Wear Properties of Their Coating, *Rare Metals.*, 2011, **30**, p 262–266
14. Y. Zhao, K. Kamiya, K. Hashimoto, and S. Nakanishi, In Situ CO_2-Emission Assisted Synthesis of Molybdenum Carbonitride Nanomaterial as Hydrogen Evolution Electrocatalyst, *J. Am. Chem. Soc.*, 2015, **137**, p 110–113
15. Z.G. Yuan, J.F. Yang, X.P. Wang, Z.J. Cheng, and Q.F. Fang, Characterization and Properties of Quaternary Mo-Si-C-N Coatings Synthesized by Magnetron Sputtering Technique, *Surf. Coat. Technol.*, 2011, **205**, p 3307–3312
16. D.V. Shtansky, A.V. Bondarev, Ph.V. Kiryukhantsev-Korneev, T.C. Rojas, V. Godinho, and A. Fernández, Structure and Tribological Properties of MoCN-Ag Coatings in the Temperature Range of 25-700 °C, *Appl. Surf. Sci.*, 2013, **273**, p 408–414
17. A.V. Bondarev, Ph.V. Kiryukhantsev-Korneev, D.A. Sidorenko, and D.V. Shtansky, A New Insight into Hard Low Friction MoCN-Ag Coatings Intended for Applications in Wide Temperature Range, *Mater. Des.*, 2016, **93**, p 63–72
18. H.-J. Butt, B. Cappella, and M. Kappl, Force Measurements with the Atomic Force Microscope: Technique, Interpretation and Applications, *Surf. Sci. Rep.*, 2005, **59**, p 1–152
19. M. Andreyev, V. Anishchik, L. Markova, and T. Kuznetsova, Ion-Beam Coatings Based on Ni and Cr with Ultradispersed Diamonds—Structure and Properties, *Vacuum*, 2005, **78**, p 451–454
20. A. Gilewicz, R. Jedrzejewski, A.E. Kochmanska, and B. Warcholinski, Structure of MoCN Films Deposited by Cathodic Arc Evaporation, *Thin Solid Films*, 2015, **577**, p 94–96
21. B. Bhushan, *Nanotribology and Nanomechanics, an Introduction*, 2nd ed., Springer, Berlin, 2008
22. A. Gilewicz, B. Warcholinski, and D. Murzynski, The Properties of Molybdenum Nitride Coatings Obtained by Cathodic Arc Evaporation, *Surf. Coat. Technol.*, 2013, **236**, p 149–158
23. H.H. Hausner, *Coatings of High-Temperature Materials*, Springer, New York, 1996